Control Engineering Practice 18 (2010) 936–943

Contents lists available at ScienceDirect

Control Engineering Practice

journal homepage: www.elsevier.com/locate/conengprac

Nonlinear adaptive model following control for a 3-DOF tandem-rotor model helicopter

Mitsuaki Ishitobi *, Masatoshi Nishi, Kazuhide Nakasaki

Department of Mechanical Systems Engineering, Kumamoto University, Kumamoto 860-8555, Japan

ARTICLE INFO

Article history:
Received 28 October 2008
Accepted 30 March 2010
Available online 28 April 2010

Keywords:
Tandem-rotor helicopters
Nonlinear control
Model following control
Adaptive control
Parameter identification

ABSTRACT

This paper considers two-input, two-output nonlinear adaptive model following control of a 3-DOF (degree-of-freedom) tandem rotor model helicopter. The control performance is studied by real time implementation of the control algorithms in an actual helicopter testbed. Since the decoupling matrix of the model helicopter is singular, the system is not decouplable by static state feedback, and it is challenging to design a feedback control system. Dynamic state feedback is applied. The controller is designed using a nonlinear structure algorithm. Furthermore, a parameter identification scheme is introduced in the closed-loop system to improve the control performance. Three identification methods are discussed.

1. Introduction

Interests in designing feedback controllers for helicopters have increased over the last 10 years or so because unmanned helicopters can remove individuals from dangerous tasks. The main difficulties in designing stable feedback controllers for helicopters arise from the high nonlinearities, cross-couplings and large uncertainty of dynamics of these aircraft. To date, various efforts have been directed to the development of effective feedback control algorithms, from classical control to advanced control, for helicopters. Among earlier works, classical SISO (single-input single-output) techniques with a PI (proportional and integral) controller are used widely (Kim, & Shim, 2003). The SISO control approaches have advantages of simple structure, straightforward design procedure and so on. It is, however, difficult to take into account of uncertainties and couplings. Hence, attention has been focused on development of MIMO (multi-input multi-output) control approaches. Among MIMO approaches, H-infinity theory has been often adopted as it provides robust stability for plants subject to uncertainties (Postlethwaite et al., 2005; Trentini, & Pieper, 2001). Sira-Ramirez, Zribi, and Ahmad (1994) have applied dynamical sliding mode control to the altitude stabilization of a nonlinear helicopter model in vertical flight. Other MIMO control approaches for tracking are investigated by Koo and Sastry (1998), Dzul, Hamel, and Lozano (2002), Hu, Zhu, Huang, Hu, and Sun (2004), Mahony and Hamel (2004), Marconi and Naldi (2007), and Chakrabortty, Arcak, and Tsiotras (2008). Adaptive control is also known as one of the control strategies to overcome an uncertainty problem (Krstic, Kanellakopolous, & Kokotovic, 1995; Tao, 2003). Kutay, Calise, Idan, and Hovakimyan (2005) have presented experimental results of a direct output feedback adaptive control method but their method is applied to an SISO model which involves only the pitch angle of a 3-DOF laboratory helicopter.

In this paper, therefore, a two-input, two-output nonlinear model following control problem of a 3-DOF tandem rotor helicopter is considered. The control performance is studied by real time implementation of the control algorithms in an actual helicopter testbed. The word 'nonlinear model following control' implies that the feedback controller causes the output of a controlled nonlinear system to track the output of a reference model. The basic idea of controller design is linearization of the input–output relationships of the system. A well-known application example of input–output linearization is motion control of a robot manipulator which is decouplable by static state feedback (Spong, Lewis, & Abdallah, 1992). However, since the decoupling matrix of the model helicopter considered is singular and the system is not decouplable by static state feedback, it is challenging to design the feedback control system. Here, a nonlinear structure algorithm (Isidori, 1995; Isurugi, 1990; Shima et al., 1997; Singh, 1981) is used to design the controller. The feedback controller based on the nonlinear structure algorithm is achieved by dynamic state feedback. Due to the fact that it is difficult to find practical application examples of a nonlinear structure algorithm in literature, the first main contribution of this paper is to show feasibility of the nonlinear structure algorithm for a model helicopter which is not decouplable by static state feedback.

* Corresponding author. Tel./fax: +81 96 342 3777.
E-mail address: mishi@kumamoto-u.ac.jp (M. Ishitobi).

0967-0661/$ - see front matter © 2010 Elsevier Ltd. All rights reserved.
doi:10.1016/j.conengprac.2010.03.017

When a simple model following controller based on the nonlinear structure algorithm is designed, it is difficult to obtain a good control performance in actual experiment mainly due to the parameter uncertainties. Fortunately, the system dynamics of the model helicopter are linear with respect to unknown parameters even though the system equations are nonlinear. Hence, first a standard identification scheme is introduced in the feedback closed-loop, but the experimental results show that the control performance is not improved satisfactorily. The main reason for the poor results is that the estimated velocity and acceleration signals are inaccurate. To obtain better performance, this paper proposes the second identification scheme which requires neither velocity nor acceleration signals. Further, the robustness problem to model uncertainties and external disturbances is also discussed.

2. System description

This paper considers a tandem rotor model helicopter of Quanser Consulting, Inc. The configuration of the model helicopter experimental system is illustrated in Fig. 1. The helicopter body is mounted at the end of an arm and is free to move about the elevation, pitch and horizontal travel axes. Thus the helicopter has 3-DOF: the elevation ε, pitch θ and travel ϕ angles, all of which are measured via optical encoders. The movement range of the elevation ε and pitch θ angles is limited between around -1 and 1 rad due to the hardware restriction. Two DC motors attached to propellers generate a driving force proportional to the voltage output of a controller.

The system dynamics are expressed by the following highly nonlinear and coupled state variable equations (Apkarian, 1998):

$$\dot{\boldsymbol{x}}_p = f(\boldsymbol{x}_p) + [g_1(\boldsymbol{x}_p), g_2(\boldsymbol{x}_p)]\boldsymbol{u}_p \tag{1}$$

where

$$\boldsymbol{x}_p = [x_{p1}, x_{p2}, x_{p3}, x_{p4}, x_{p5}, x_{p6}]^T = [\varepsilon, \dot{\varepsilon}, \theta, \dot{\theta}, \phi, \dot{\phi}]^T$$

$$\boldsymbol{u}_p = [u_{p1}, u_{p2}]^T$$

$$u_{p1} = V_f + V_b, \quad u_{p2} = V_f - V_b$$

$$f(\boldsymbol{x}_p) = \begin{bmatrix} \dot{\varepsilon} \\ p_1\cos\varepsilon + p_2\sin\varepsilon + p_3\dot{\varepsilon} \\ \dot{\theta} \\ p_5\cos\theta + p_6\sin\theta + p_7\dot{\theta} \\ \dot{\phi} \\ p_9\dot{\phi} \end{bmatrix}$$

$$g_1(\boldsymbol{x}_p) = [0, p_4\cos\theta, 0, 0, 0, p_{10}\sin\theta]^T$$

$$g_2(\boldsymbol{x}_p) = [0, 0, 0, p_8, 0, 0]^T$$

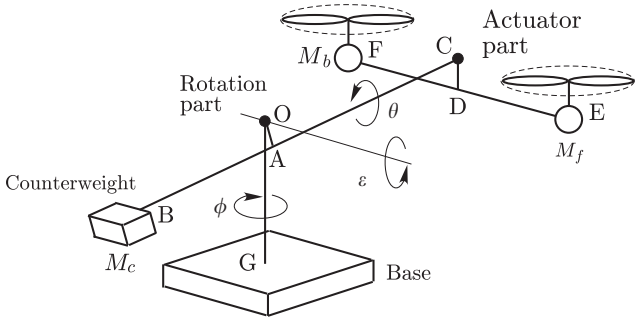

Fig. 1. Configuration of the model helicopter experimental system.

$$p_1 = [-(M_f + M_b)gL_a + M_c gL_c]/J_\varepsilon$$

$$p_2 = -[(M_f + M_b)gL_a\tan\delta_a + M_c gL_c\tan\delta_c]/J_\varepsilon$$

$$p_3 = -\eta_\varepsilon/J_\varepsilon, \quad p_4 = K_m L_a/J_\varepsilon$$

$$p_5 = (-M_f + M_b)gL_h/J_\theta$$

$$p_6 = -(M_f + M_b)gL_h\tan\delta_h/J_\theta$$

$$p_7 = -\eta_\theta/J_\theta, \quad p_8 = K_m L_h/J_\theta$$

$$p_9 = -\eta_\phi/J_\phi, \quad p_{10} = -K_m L_a/J_\phi$$

$$\delta_a = \tan^{-1}\{(L_d + L_e)/L_a\}$$

$$\delta_c = \tan^{-1}(L_d/L_c)$$

$$\delta_h = \tan^{-1}(L_e/L_h)$$

The notation employed above is defined as follows:

V_f, V_b (V) voltage applied to the front motor, voltage applied to the rear motor,
M_f, M_b (kg) mass of the front section of the helicopter, mass of the rear section,
M_c (kg) mass of the counterbalance,
L_d, L_c, L_a, L_e, L_h (m) distances OA, AB, AC, CD, DE=DF,
g (m/s^2) gravitational acceleration,
$J_\varepsilon, J_\theta, J_\phi$ (kg m^2) moment of inertia about the elevation, pitch and travel axes,
$\eta_\varepsilon, \eta_\theta, \eta_\phi$ (kg m^2/s) coefficient of viscous friction about the elevation, pitch and travel axes.

The forces of the front and rear rotors are assumed to be $F_f = K_m V_f$, $F_b = K_m V_b$ (N), respectively, where K_m (N/V) is a force constant.

It may be noted that all the parameters p_i $(i = 1 \ldots 10)$ are constants.

For the problem of the control of the position of the model helicopter, two angles, the elevation ε and the travel ϕ angles, are selected as the outputs from the three detected signals of the three angles. Hence, one has

$$\boldsymbol{y}_p = [\varepsilon, \phi]^T \tag{2}$$

Differentiating the output $\boldsymbol{y}_p$ twice leads to the following decoupling matrix:

$$B(\boldsymbol{x}) = \begin{bmatrix} p_4\cos x_{p3} & 0 \\ p_{10}\sin x_{p3} & 0 \end{bmatrix} \tag{3}$$

which is obviously singular. Hence, the system is not decouplable by static state feedback (Isidori, 1995; Shima et al., 1997).

3. Control system design

In this section, a nonlinear model following control system is designed for the 3-DOF model helicopter described in the previous section.

3.1. Reference model

First, the reference model is given as

$$\dot{\boldsymbol{x}}_M = A_M\boldsymbol{x}_M + B_M\boldsymbol{u}_M, \quad \boldsymbol{y}_M = C_M\boldsymbol{x}_M$$

$$\boldsymbol{x}_M = [x_{M1}, x_{M2}, x_{M3}, x_{M4}, x_{M5}, x_{M6}, x_{M7}, x_{M8}]^T = [\varepsilon_M, \dot{\varepsilon}_M, \ddot{\varepsilon}_M, \varepsilon_M^{(3)}, \phi_M, \dot{\phi}_M, \ddot{\phi}_M, \phi_M^{(3)}]^T$$

$$\boldsymbol{y}_M=[\varepsilon_M,\phi_M]^T,\quad \boldsymbol{u}_M=[u_{M1},u_{M2}]^T \tag{4}$$

where

$$A_M=\begin{bmatrix}K_1 & 0\\ 0 & K_2\end{bmatrix},\quad B_M=\begin{bmatrix}\boldsymbol{i}_1 & \boldsymbol{0}\\ \boldsymbol{0} & \boldsymbol{i}_1\end{bmatrix},\quad C_M=\begin{bmatrix}\boldsymbol{i}_2^T & \boldsymbol{0}^T\\ \boldsymbol{0}^T & \boldsymbol{i}_2^T\end{bmatrix}$$

$$K_i=\begin{bmatrix}0 & 1 & 0 & 0\\ 0 & 0 & 1 & 0\\ 0 & 0 & 0 & 1\\ k_{i1} & k_{i2} & k_{i3} & k_{i4}\end{bmatrix},\quad \boldsymbol{i}_1=\begin{bmatrix}0\\0\\0\\1\end{bmatrix},\quad \boldsymbol{i}_2=\begin{bmatrix}1\\0\\0\\0\end{bmatrix}$$

Since cross-coupling is one of the main difficulties in designing feedback controllers for helicopters, the reference model is here given so as to achieve decoupling. The reference model has two more states than the plant so that the feedback inputs do not include the derivatives of the reference inputs $\boldsymbol{u}_M$ as one can see in Section 3.2.

3.2. Model following control by the nonlinear structure algorithm

This subsection explains a model following controller design based on the nonlinear structure algorithm.

From Eqs. (1) and (4), the augmented state equation is defined as follows:

$$\dot{\boldsymbol{x}}=f(\boldsymbol{x})+G(\boldsymbol{x})\boldsymbol{u}$$

$$\boldsymbol{x}=[\boldsymbol{x}_p^T,\boldsymbol{x}_M^T]^T,\quad \boldsymbol{u}=[\boldsymbol{u}_p^T,\boldsymbol{u}_M^T]^T$$

$$f(\boldsymbol{x})=\begin{bmatrix}f(\boldsymbol{x}_p)\\ A_M\boldsymbol{x}_M\end{bmatrix},\quad G(\boldsymbol{x})=\begin{bmatrix}g_1(\boldsymbol{x}_p) & g_2(\boldsymbol{x}_p) & O\\ \boldsymbol{0} & \boldsymbol{0} & B_M\end{bmatrix} \tag{5}$$

Here, a nonlinear structure algorithm is applied to design a model following controller (Isidori, 1995; Isurugi, 1990; Shima et al., 1997; Singh, 1981). In the nonlinear structure algorithm, elimination of one of inputs and differentiating of the error equation are repeated until a nonsingular decoupling matrix is obtained. New variables and parameters in the following algorithm are defined below the input (13).

- *Step* 1: First, a tracking error vector is defined by

$$\boldsymbol{e}=\begin{bmatrix}e_1\\ e_2\end{bmatrix}=\begin{bmatrix}x_{M1}-x_{p1}\\ x_{M5}-x_{p5}\end{bmatrix} \tag{6}$$

Differentiating the tracking error (6) yields

$$\dot{\boldsymbol{e}}=\frac{\partial \boldsymbol{e}}{\partial \boldsymbol{x}}\{f(\boldsymbol{x})+G(\boldsymbol{x})\boldsymbol{u}\}=\begin{bmatrix}-x_{p2}+x_{M2}\\ -x_{p6}+x_{M6}\end{bmatrix} \tag{7}$$

Since the inputs do not appear in Eq. (7), one proceeds to step 2.

- *Step* 2: Differentiating Eq. (7) leads to

$$\ddot{\boldsymbol{e}}=\begin{bmatrix}r_1(\boldsymbol{x})\\ -p_9x_{p6}+x_{M7}\end{bmatrix}+[B_u(\boldsymbol{x}),B_r(\boldsymbol{x})]\boldsymbol{u}$$

$$B_u(\boldsymbol{x})=\begin{bmatrix}-p_4\cos x_{p3} & 0\\ -p_{10}\sin x_{p3} & 0\end{bmatrix},\quad B_r(\boldsymbol{x})=O \tag{8}$$

From Eq. (8), the decoupling matrix $B_u(\boldsymbol{x})$ is singular. Hence, this system is not decouplable by static state feedback (Isidori, 1995; Shima et al., 1997). According to the nonlinear structure algorithm, elimination of one of inputs and differentiating of the error equation are repeated until a nonsingular decoupling matrix appears. Hence, by eliminating u_{p1} from Eq. (8) under the assumption of $u_{p1}\neq 0$, one obtains

$$\ddot{e}_2=-p_9x_{p6}+x_{M7}+p_{14}\tan x_{p3}(\ddot{e}_1-r_1(\boldsymbol{x})) \tag{9}$$

- *Step* 3: Further differentiating Eq. (9) gives rise to

$$\begin{aligned}e_2^{(3)}=&\,p_{14}\tan x_{p3}\{d_5(\boldsymbol{x})x_{p2}+p_3(x_{M3}-r_1(\boldsymbol{x}))+x_{M4}+e_1^{(3)}\}\\ &-d_4(\boldsymbol{x})r_1(\boldsymbol{x})x_{p4}-p_9^2x_{p6}+x_{M8}+[p_{10}\sin x_{p3}(p_3-p_9),0,0,0]\boldsymbol{u}\end{aligned} \tag{10}$$

As well as step 2, one eliminates u_{p1} from Eqs. (8) and (10), and it is obtained that

$$\begin{aligned}e_2^{(3)}=&\,p_{14}\tan x_{p3}\{p_3x_{M3}-d_5(\boldsymbol{x})-p_3r_1(\boldsymbol{x})-x_{M4}+e_1^{(3)}\\ &-p_{15}\ddot{e}_1+p_{15}r_1(\boldsymbol{x})\}+x_{M8}-p_9^2x_{x6}-d_4(\boldsymbol{x})x_{p4}r_1(\boldsymbol{x})\end{aligned} \tag{11}$$

- *Step* 4: It follows from the same operation as step 3 that

$$e_2^{(4)}=r_2(\boldsymbol{x})+[d_1(\boldsymbol{x}),d_2(\boldsymbol{x}),d_3(\boldsymbol{x}),1]\boldsymbol{u} \tag{12}$$

From Eqs. (8) and (12), the system is input–output linearizable (Isidori, 1995; Shima et al., 1997) and the model following input vector is determined as

$$\boldsymbol{u}_p=R(\boldsymbol{x})+S(\boldsymbol{x})\boldsymbol{u}_M$$

$$R(\boldsymbol{x})=\frac{1}{d_2(\boldsymbol{x})p_4\cos x_{p3}}\begin{bmatrix}-d_2(\boldsymbol{x}) & 0\\ d_1(\boldsymbol{x}) & p_4\cos x_{p3}\end{bmatrix}\begin{bmatrix}\bar{e}_1-r_1(\boldsymbol{x})\\ \bar{e}_2-r_2(\boldsymbol{x})\end{bmatrix}$$

$$S(\boldsymbol{x})=\frac{-1}{d_2(\boldsymbol{x})p_4\cos x_{p3}}\begin{bmatrix}-d_2(\boldsymbol{x}) & 0\\ d_1(\boldsymbol{x}) & p_4\cos x_{p3}\end{bmatrix}\begin{bmatrix}0 & 0\\ d_3(\boldsymbol{x}) & 1\end{bmatrix} \tag{13}$$

where

$$\bar{e}_1=-\sigma_{12}\dot{e}_1-\sigma_{11}e_1$$

$$\bar{e}_2=-\sigma_{24}e_2^{(3)}-\sigma_{23}\ddot{e}_2-\sigma_{22}\dot{e}_2-\sigma_{21}e_2$$

$$r_1(\boldsymbol{x})=-p_1\cos x_{p1}-p_2\sin x_{p1}-p_3x_{p2}+x_{M3}$$

$$\begin{aligned}r_2(\boldsymbol{x})=&\{-d_5(\boldsymbol{x})(p_9p_{14}\tan x_{p3}+x_{p4}d_4(\boldsymbol{x}))-p_{14}x_{p2}\tan x_{p3}(p_1\cos x_{p1}\\ &+p_2\sin x_{p1})\}x_{p2}+\{p_3x_{p4}d_4(\boldsymbol{x})+p_{14}\tan x_{p3}(p_3p_9\\ &-d_5(\boldsymbol{x}))\}(x_{M3}-r_1(\boldsymbol{x}))+\{p_3(x_{M3}-r_1(\boldsymbol{x}))\\ &+(2x_{p4}\tan x_{p3}-p_{15})(\ddot{e}_1-r_1(\boldsymbol{x}))-x_{M4}\\ &+e_1^{(3)}-x_{p2}d_5(\boldsymbol{x})\}x_{p4}d_4(\boldsymbol{x})+(\ddot{e}_1-r_1(\boldsymbol{x}))(p_5\cos x_{p3}\\ &+p_6\sin x_{p3}+p_7x_{p4})d_4(\boldsymbol{x})+(x_{p4}d_4(\boldsymbol{x})-p_{14}p_{15}\tan x_{p3})e_1^{(3)}\\ &+p_{14}\tan x_{p3}(p_{15}x_{M4}-k_1x_{M1}-k_2x_{M2}-k_3x_{M3}-k_4x_{M4})\\ &-x_{p4}x_{M4}d_4(\boldsymbol{x})+k_5x_{M5}+k_6x_{M6}+k_7x_{M7}+k_8x_{M8}\\ &+p_{14}e_1^{(4)}\tan x_{p3}-p_9^3x_{p6}\end{aligned}$$

$$d_1(\boldsymbol{x})=(p_3p_9-d_5(\boldsymbol{x})-p_9^2)p_{10}\sin x_{p3}+p_3p_4x_{p4}d_4(\boldsymbol{x})\cos x_{p3}$$

$$d_2(\boldsymbol{x})=p_8d_4(\boldsymbol{x})(\ddot{e}_1-r_1(\boldsymbol{x}))$$

$$d_3(\boldsymbol{x})=-p_{14}\tan x_{p3}$$

$$d_4(\boldsymbol{x})=\frac{p_{14}}{\cos^2 x_{p3}}$$

$$d_5(\boldsymbol{x})=p_1\sin x_{p1}-p_2\cos x_{p1}$$

$$e_1=x_{M1}-x_{p1}$$

$$\dot{e}_1=x_{M2}-x_{p2}$$

$$\ddot{e}_1=-\sigma_{12}\dot{e}_1-\sigma_{11}e_1$$

$$e_1^{(3)}=(\sigma_{12}^2-\sigma_{11})\dot{e}_1+\sigma_{12}\sigma_{11}e_1$$

$$e_1^{(4)}=(-\sigma_{12}^3+2\sigma_{12}\sigma_{11})\dot{e}_1-\sigma_{11}(\sigma_{12}^2-\sigma_{11})e_1$$

$$e_2 = x_{M5} - x_{p5}, \quad \dot{e}_2 = x_{M6} - x_{p6}$$

$$\ddot{e}_2 = p_{14}\tan x_{p3}(\ddot{e}_1 - r_1(\boldsymbol{x})) - p_9 x_{p6} + x_{M7}$$

$$e_2^{(3)} = p_{14}\tan x_{p3}\{p_3(x_{M3} - r_1(\boldsymbol{x})) - x_{p2}d_5(\boldsymbol{x}) + e_1^{(3)} + p_{15}(r_1(\boldsymbol{x}) - \ddot{e}_1) - x_{M4}\} + x_{M8} + x_{p4}d_4(\boldsymbol{x})(\ddot{e}_1 - r_1(\boldsymbol{x})) - (p_9^2 x_{p_\varepsilon})$$

$$p_{14} = \frac{p_{10}}{p_4}$$

$$p_{15} = p_3 - p_9$$

The input vector is always available since the term $d_2(\boldsymbol{x})\cos x_{p3}$ does not vanish for $-\pi/2 < \theta < \pi/2$. The design parameters σ_{ij} $(i = 1,2, j = 1,\ldots,4)$ are selected so that the characteristic equations $\lambda^2 + \sigma_{12}\lambda + \sigma_{11} = 0$ and $\lambda^4 + \sigma_{24}\lambda^3 + \sigma_{23}\lambda^2 + \sigma_{22}\lambda + \sigma_{21} = 0$ are stable. Then, the closed-loop system has the following error equations:

$$\ddot{e}_1 + \sigma_{12}\dot{e}_1 + \sigma_{11}e_1 = 0 \tag{14}$$

$$e_2^{(4)} + \sigma_{24}e_2^{(3)} + \sigma_{23}\ddot{e}_2 + \sigma_{22}\dot{e}_2 + \sigma_{21}e_2 = 0 \tag{15}$$

and the plant outputs converge to the reference outputs. From Eqs. (8) and (12), u_{p1} and u_{p2} appear first in $\ddot{e}_1$ and $e_2^{(4)}$, respectively. Thus, there are no zero dynamics and the system is minimum phase since the order of Eq. (1) is six (Isidori, 1995; Shima et al., 1997). Further, one can see that the order of the reference model should be eight so that the inputs (13) do not include the derivatives of the reference inputs $\boldsymbol{u}_M$.

3.3. Velocity signals

Since the controller requires the angular velocity signals $\dot{\varepsilon}, \dot{\theta}$ and $\dot{\phi}$, in the experiment these signals are calculated numerically from the measured angular positions by a discretized differentiator with the first-order filter

$$H_l(z) = \frac{\alpha(1 - z^{-1})}{1 - z^{-1} + \alpha T_s} \tag{16}$$

which is derived by substituting $s = (1 - z^{-1})/T_s$ into the differentiator $G_l(s) = \alpha s/(s + \alpha)$, where z^{-1} is a one-step delay operator, T_s is the sampling period and the design parameter α is a positive constant. Hence, for example, one has

$$\dot{\varepsilon}(k) \approx \frac{1}{\alpha T_s + 1}[\dot{\varepsilon}(k-1) + \alpha\{\varepsilon(k) - \varepsilon(k-1)\}] \tag{17}$$

4. Parameter identification based on the differential equations

4.1. Parameter identification algorithm

It is difficult to obtain the desired control performance by applying the above algorithm directly to the experimental system, since there are parameter uncertainties in the model dynamics. However, it is straightforward to see that the system dynamics (1) are linear with respect to unknown parameters, even though the equations are nonlinear. It is therefore possible to introduce a parameter identification scheme in the feedback control loop.

In the present study, the parameter identification scheme is designed in discrete-time form using measured discrete-time signals. Hence, the estimated parameters are calculated recursively at every instant kT, where T is the updating period of the parameters and k is a nonnegative integer. Henceforth T is omitted for simplicity in the identification algorithm. Further, the indirect identification method is here considered since the direct law needs much more identification parameters and the structure of the identifier is very complicated. Then, the dynamics of the model helicopter given by Eq. (1) can be re-expressed as

$$w_1(k) \equiv \ddot{\varepsilon}(k) = \zeta_1^T \boldsymbol{v}_1(k), \quad w_2(k) \equiv \ddot{\theta}(k) = \zeta_2^T \boldsymbol{v}_2(k)$$

$$w_3(k) \equiv \ddot{\phi}(k) = \zeta_3^T \boldsymbol{v}_3(k) \tag{18}$$

where

$$\zeta_1 = [p_1, p_2, p_3, p_4]^T$$

$$\zeta_2 = [p_5, p_6, p_7, p_8]^T, \quad \zeta_3 = [p_9, p_{10}]^T$$

$$\boldsymbol{v}_1(k) = [v_{11}(k), \ldots, v_{14}(k)]^T,$$

$$\boldsymbol{v}_2(k) = [v_{21}(k), \ldots, v_{24}(k)]^T, \quad \boldsymbol{v}_3(k) = [v_{31}(k), v_{32}(k)]^T$$

$$v_{11}(k) = \cos\varepsilon(k), \quad v_{12}(k) = \sin\varepsilon(k), \quad v_{13}(k) = \dot{\varepsilon}(k)$$

$$v_{14}(k) = u_{p1}\cos\theta(k), \quad v_{21}(k) = \cos\theta(k)$$

$$v_{22}(k) = \sin\theta(k), \quad v_{23}(k) = \dot{\theta}(k), \quad v_{24}(k) = u_{p2}(k)$$

$$v_{31}(k) = \dot{\phi}(k), \quad v_{32}(k) = u_{p1}\sin\theta(k)$$

Defining the estimated parameter vectors corresponding to the vectors $\zeta_1, \zeta_2, \zeta_3$ as $\hat{\zeta}_1(k), \hat{\zeta}_2(k), \hat{\zeta}_3(k)$, the estimated values of $w_1(k)$, $w_2(k)$, $w_3(k)$ are obtained as

$$\hat{w}_i(k) = \hat{\zeta}_i^T(k)\boldsymbol{v}_i(k), \quad i = 1,2,3 \tag{19}$$

respectively. Along with the angular velocities, the angular accelerations $w_1(k) = \ddot{\varepsilon}(k)$, $w_2(k) = \ddot{\theta}(k)$, $w_3(k) = \ddot{\phi}(k)$ are also obtained by numerical calculation using a discretized differentiator.

The parameters are estimated using a recursive least squares algorithm as follows:

$$\hat{\zeta}_i(k) = \hat{\zeta}_i(k-1) + \frac{P_i(k-1)\boldsymbol{v}_i(k-1)[w_i(k-1) - \hat{w}_i(k-1)]}{\lambda_i(k-1) + \boldsymbol{v}_i^T(k-1)P_i(k-1)\boldsymbol{v}_i(k-1)} \tag{20}$$

$$P_i^{-1}(k) = \lambda_i(k-1)P_i^{-1}(k-1) + \boldsymbol{v}_i(k-1)\boldsymbol{v}_i^T(k-1)$$
$$P_i^{-1}(0) > 0, \quad 0 < \lambda_i(k-1) \le 1, \; i = 1,2,3 \tag{21}$$

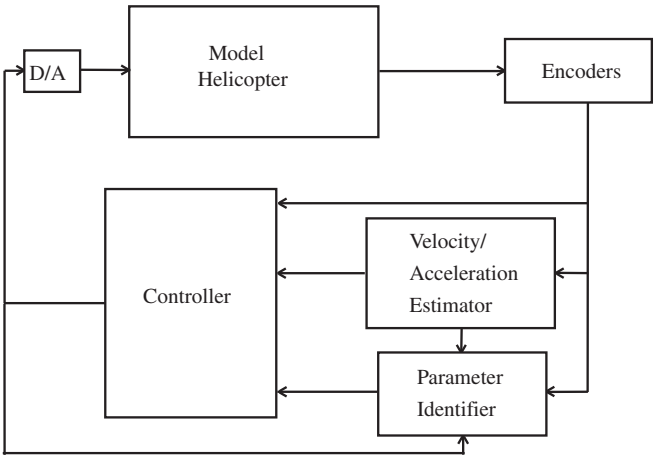

Fig. 2. Block diagram of the feedback control system.

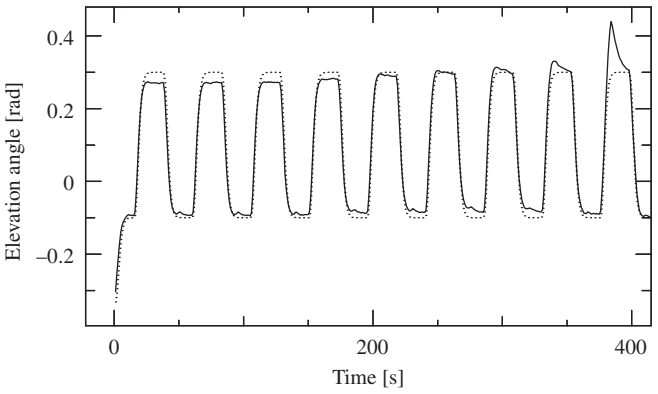

Fig. 3. Time evolution of angle ε (—) and reference output ε_M (···).

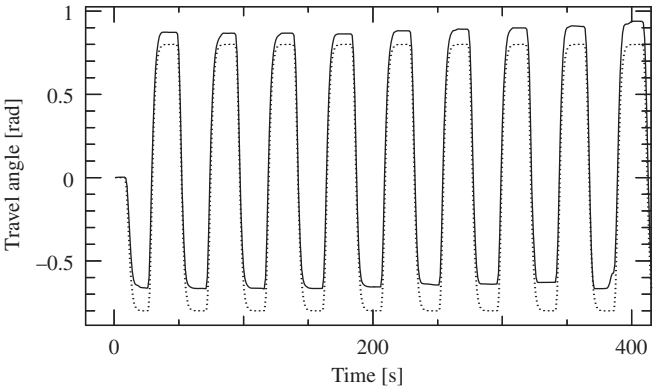

Fig. 4. Time evolution of angle ϕ (—) and reference output ϕ_M (···).

Then, the tracking of the two outputs is achieved under the persistent excitation of the signals $\boldsymbol{v}_i$.

4.2. Experimental studies

The estimation and control algorithm described above was applied to the actual experimental system shown in Section 2. The block diagram of the feedback control system is illustrated in Fig. 2. The controller is a digital computer with a Pentium 4, 2.2 GHz CPU. The software consists of the OS of Windows 2000 and of the Matlab Simulink. The angles ε, θ and ϕ are detected by encoders with 12, 12 and 13 bits, respectively. The voltages V_f and V_b of two motors are in the range (0, 5) V. The nominal values of the physical constants in the actual helicopter testbed are as follows:

$$J_\varepsilon = 0.86\,\mathrm{kg\,m^2},\quad J_\theta = 0.044\,\mathrm{kg\,m^2},\quad J_\phi = 0.82\,\mathrm{kg\,m^2},$$

$$L_a = 0.62\,\mathrm{m},\quad L_c = 0.44\,\mathrm{m},$$

$$L_d = 0.05\,\mathrm{m},\quad L_e = 0.02\,\mathrm{m},\quad L_h = 0.177\,\mathrm{m},\quad M_f = 0.69\,\mathrm{kg},$$
$$M_b = 0.69\,\mathrm{kg},$$

$$M_c = 1.67\,\mathrm{kg},\quad K_m = 0.5\,\mathrm{N/V},\quad g = 9.81\,\mathrm{m/s^2},\quad \eta_\varepsilon = 0.001\,\mathrm{kg\,m^2/s},$$

$$\eta_\theta = 0.001\,\mathrm{kg\,m^2/s},\quad \eta_\phi = 0.005\,\mathrm{kg\,m^2/s}.$$

The design parameters are given as follows: the sampling period of the inputs and the outputs is set as $T_s = 2$ ms and the updating period of the parameters takes $T = 10$ ms. Further, the filter parameter in Eq. (17) is given as $\alpha = 1000$ for the estimation of velocities and accelerations. The variation ranges of the identified parameters are restricted as

$$-1.8 \le \hat{p}_1 \le -0.8,\quad -2.2 \le \hat{p}_2 \le -1.2$$

$$-0.3 \le \hat{p}_3 \le 0.0,\quad 0.1 \le \hat{p}_4 \le 0.6$$

$$-0.5 \le \hat{p}_5 \le 0.5,\quad -7.0 \le \hat{p}_6 \le -5.2$$

$$-0.6 \le \hat{p}_7 \le 0.0,\quad 1.8 \le \hat{p}_8 \le 2.2$$

$$-0.5 \le \hat{p}_9 \le 0.0,\quad -0.5 \le \hat{p}_{10} \le -0.2 \qquad (22)$$

The forgetting factor of the least squares algorithm is given by

$$\lambda_i = 0.9995 + 0.0005\exp(-5\sqrt{e_1^2+e_2^2}),\quad i = 1,2,3$$

The introduction of the variable forgetting factor is based on the fact that it improves the accuracy of parameter identification and control performance (Goodwin, & Sin, 1984). The inputs $u_{M\,1}$ and $u_{M\,2}$ of the reference model are given by

$$u_{M1} = \begin{cases} 0.3, & 45k-30 \le t < 45k-7.5 \\ -0.1, & 45k-7.5 \le t < 45k+15 \end{cases}$$

$$u_{M2} = \begin{cases} 0, & 0 \le t < 7.5, \\ -0.8, & 45k+7.5 \le t < 45k+30, \\ 0.8, & 45k+30 \le t < 45(k+1)+7.5, \end{cases} \qquad k = 0,1,2,\ldots \qquad (23)$$

All the eigenvalues of the matrices K_1 and K_2 are -1, and the characteristic roots of the error equations (14) and (15) are specified as $(-2.0,-3.0)$ and $(-2.0,-2.2,-2.4,-2.6)$, respectively. The origin of the elevation angle ε is set as a nearly horizontal level, so the initial angle is $\varepsilon = -0.336$ rad when the voltages of two motors are zero, i.e., $V_f = V_b = 0$.

The values of the design parameters above are chosen by mainly trial and error. The selection of the sampling period T_s of the input and output is most important. The achievable minimum sampling period T_s is 2 ms due to the calculation ability of the computer. The longer it is, the worse the tracking control performance is. On the other hand, the preliminary experimental studies show that a short updating period T of the parameter estimation increases the effect of the output noise on the estimated parameters. Therefore, the updating period of the parameter is selected as $T = 10$ ms by trial and error.

The outputs of the experimental results are shown in Figs. 3 and 4. The tracking is incomplete because neither of the output errors vanishes. Fig. 5 displays the estimated parameter $\hat{p}_1$. All of the other estimated parameters move to the limiting values of the variation range as well as $\hat{p}_1$.

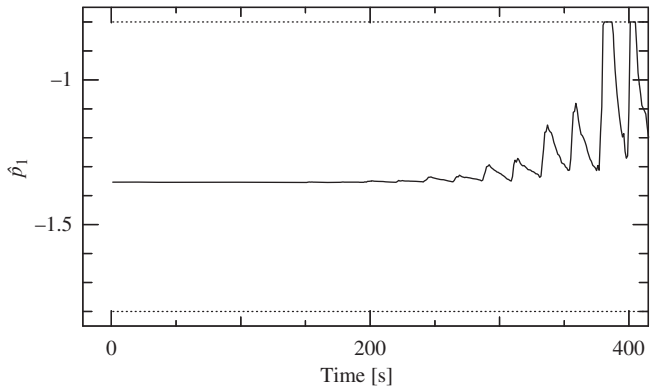

Fig. 5. Time evolution of the estimated parameter $\hat{p}_1$. The dotted lines represent the limiting values.

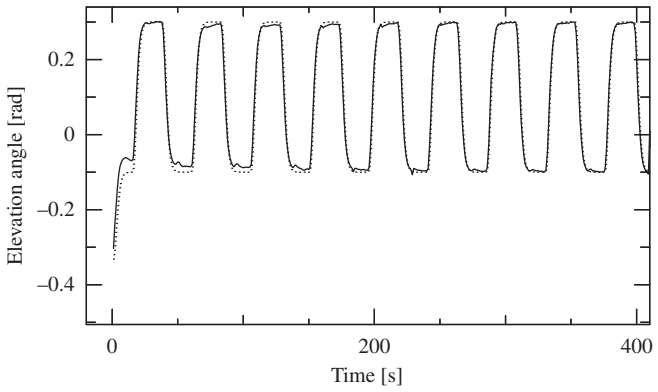

Fig. 6. Time evolution of angle ε (—) and reference output ε_M ($\cdots$).

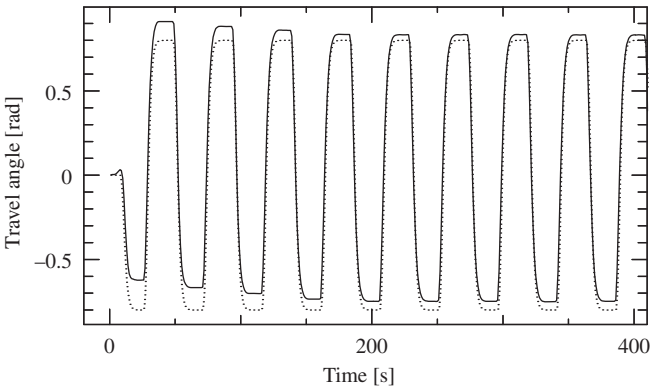

Fig. 7. Time evolution of angle ϕ (—) and reference output ϕ_M ($\cdots$).

5. Parameter identification based on the integral form of the model equations

5.1. The model equations

5.1.1. Parameter identification algorithm

The main reason why the experimental results exhibit the poor tracking performance described in Section 4.2 lies in the fact that the parameter identification is unsatisfactory due to the inaccuracy of the estimation of the velocity and the acceleration signals, for instance, $\dot{\varepsilon}(k)$ and $\ddot{\varepsilon}(k)$, equivalently $w_1(k)$ and $\hat{w}_1(k)$ obtained using the discretized differentiator. To overcome this problem in this subsection, a parameter estimation scheme is designed for modified dynamics equations obtained by applying integral operators to the differential equations expressing the system dynamics (18). Neither velocities nor accelerations appear in these modified equations.

Define $\overline{w}_1(k)$ by the following double integral:

$$\overline{w}_1(k) \equiv \int_{kT-nT}^{kT} \int_{\tau-nT}^{\tau} \ddot{\varepsilon}(\sigma)\, d\sigma\, d\tau \tag{24}$$

Then, the direct calculation of the right-hand side of Eq. (24) leads to

$$\begin{aligned}\int_{kT-nT}^{kT} \int_{\tau-nT}^{\tau} \ddot{\varepsilon}(\sigma)\, d\sigma\, d\tau &= \int_{kT-nT}^{kT} (\dot{\varepsilon}(\tau)-\dot{\varepsilon}(\tau-nT))\, d\tau \\ &= \varepsilon(kT)-2\varepsilon(kT-nT)+\varepsilon(kT-2nT)\end{aligned} \tag{25}$$

Next, discretizing the double integral of the right-hand side of Eq. (18) yields

$$\begin{aligned}&p_1 \int_{kT-nT}^{kT} \int_{\tau-nT}^{\tau} \cos\varepsilon(\sigma)\, d\sigma\, d\tau + \cdots + p_3 \int_{kT-nT}^{kT} \{\varepsilon(\tau)-\varepsilon(\tau-nT)\}\, d\tau + \cdots \\ &\quad \approx p_1 T^2 \sum_{l=k-(n-1)}^{k} \sum_{i=l-(n-1)}^{l} \cos\varepsilon(i) + \cdots \\ &\quad + p_3 T \sum_{l=k-(n-1)}^{k} \{\varepsilon(l)-\varepsilon(l-(n-1))\} + \cdots\end{aligned} \tag{26}$$

As a result, the integral form of the dynamics is obtained as

$$\overline{w}_i(k) = \zeta_i^T \overline{\boldsymbol{v}}_i(k), \quad i = 1,2,3 \tag{27}$$

where

$$\overline{w}_2(k) \equiv \theta(k)-2\theta(k-n)+\theta(k-2n) \tag{28}$$

$$\overline{w}_3(k) \equiv \phi(k)-2\phi(k-n)+\phi(k-2n) \tag{29}$$

$$\overline{\boldsymbol{v}}_1(k) = [\overline{v}_{11}(k), \ldots, \overline{v}_{14}(k)]^T$$

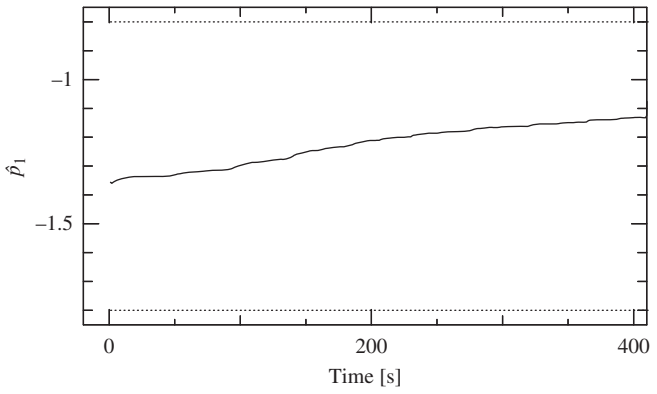

Fig. 8. Time evolution of the estimated parameter $\hat{p}_1$. The dotted lines represent the limiting values.

$$\overline{\boldsymbol{v}}_2(k) = [\overline{v}_{21}(k), \ldots, \overline{v}_{24}(k)]^T, \quad \overline{\boldsymbol{v}}_3(k) = [\overline{v}_{31}(k), \overline{v}_{32}(k)]^T$$

$$\tilde{v}_{13}(l) \equiv \varepsilon(l)-\varepsilon(l-(n-1))$$

$$\tilde{v}_{23}(l) \equiv \theta(l)-\theta(l-(n-1))$$

$$\tilde{v}_{31}(l) \equiv \phi(l)-\phi(l-(n-1))$$

$$\overline{v}_{ij}(k) = \sum_{l=k-(n-1)}^{k} \tilde{v}_{ij}(l) \quad (i,j) = \{(1,3),(2,3),(3,1)\}$$

$$\overline{v}_{ij}(k) = \sum_{l=k-(n-1),\, m=l-(n-1)}^{k} \sum^{l} v_{ij}(m) \quad \text{for other } i,j$$

Hence, the estimate model for Eq. (27) is given by

$$\hat{\overline{w}}_i(k) = \hat{\zeta}_i^T(k) \overline{\boldsymbol{v}}_i(k), \quad i = 1,2,3 \tag{30}$$

and the system parameters $\hat{\zeta}_i^T(k)$ can be identified on the basis of the expression (30) without use of the velocities or accelerations of ε, θ, ϕ.

Finally, the same parameter identification algorithm as (20) and (21) is applied to the estimate model (30).

Note here that the estimated velocity and acceleration signals are still used in the control input (13).

5.1.2. Experimental studies

As well as Section 4.2, the estimation and control algorithm described above was applied to the experimental system shown

in Section 2. The design parameter for the integral form of the identification algorithm is given by $n=100$. The other parameters, the reference model and the reference input are the same as those of the previous section. The outputs are shown in Figs. 6 and 7. The tracking performance of both the outputs ε and ϕ is improved in comparison with the previous section. However, there still remains a tracking error. The estimated parameter $\hat{p}_1$ is plotted in Fig. 8. It changes slowly, and the variation of the estimated parameter in Fig. 8 is smaller than that of the corresponding value shown in Fig. 5.

5.2. The model equations with model uncertainties and external disturbances

5.2.1. Parameter identification algorithm

Although the use of the integral form of the dynamics has improved the tracking performance of both the outputs ε and θ, tracking errors still remain. Since it seems that these errors are caused by model uncertainties and external disturbances, for example, motor dynamics or friction (other than viscous friction), one may add the extra terms M_ε, M_θ and M_ϕ into Eq. (1) to represent model uncertainties and external disturbances. Generally, the extra terms should be given as, for instance,

$$M_\varepsilon(t)=\sum_{i=1}^{\ell_\varepsilon} c_i M_i(t) \tag{31}$$

where c_i is a constant and $M_i(t)$ is a known function of time. For simplicity, however, here it is assumed that these extra terms are constant because tracking errors in the experimental results approximately remain constant in Section 5.1.2. Then, the system dynamics are expressed as

$$w_1(k)\equiv\ddot{\varepsilon}(k)=\boldsymbol{\xi}_1^T\boldsymbol{q}_1(k),\quad w_2(k)\equiv\ddot{\theta}(k)=\boldsymbol{\xi}_2^T\boldsymbol{q}_2(k)$$

$$w_3(k)\equiv\ddot{\phi}(k)=\boldsymbol{\xi}_3^T\boldsymbol{q}_3(k) \tag{32}$$

where

$$\boldsymbol{\xi}_1=[\boldsymbol{\zeta}_1^T,p_{11}]^T,\quad \boldsymbol{\xi}_2=[\boldsymbol{\zeta}_2^T,p_{12}]^T$$

$$\boldsymbol{\xi}_3=[\boldsymbol{\zeta}_3^T,p_{13}]^T,\quad \boldsymbol{q}_1(k)=[\boldsymbol{v}_1^T(k),1]^T$$

$$\boldsymbol{q}_2(k)=[\boldsymbol{v}_2^T(k),1]^T,\quad \boldsymbol{q}_3(k)=[\boldsymbol{v}_3^T(k),1]^T$$

$$p_{11}=M_\varepsilon/J_\varepsilon,\quad p_{12}=M_\theta/J_\theta,\quad p_{13}=M_\phi/J_\phi$$

It is worth noting that all the parameters p_i ($i=11,\ldots,13$) of the equations are constant. Then, the integral form of the dynamics is obtained as well as the previous subsection as

$$z_i(k)=\boldsymbol{\xi}_i^T\overline{\boldsymbol{q}}_i(k),\quad i=1,2,3 \tag{33}$$

where

$$\overline{\boldsymbol{q}}_1(k)=[\overline{\boldsymbol{v}}_1^T(k),T^2(n-1)^2]^T,\quad \overline{\boldsymbol{q}}_2(k)=[\overline{\boldsymbol{v}}_2^T(k),T^2(n-1)^2]^T$$

$$\overline{\boldsymbol{q}}_3(k)=[\overline{\boldsymbol{v}}_3^T(k),T^2(n-1)^2]^T$$

Hence, defining the estimated parameter vectors corresponding to the vectors ξ_1,ξ_2,ξ_3 as $\hat{\xi}_1(k)$, $\hat{\xi}_2(k)$, $\hat{\xi}_3(k)$, the estimate model for expression (33) is given by

$$\hat{z}_i(k)=\hat{\boldsymbol{\xi}}_i^T(k)\overline{\boldsymbol{q}}_i(k),\quad i=1,2,3 \tag{34}$$

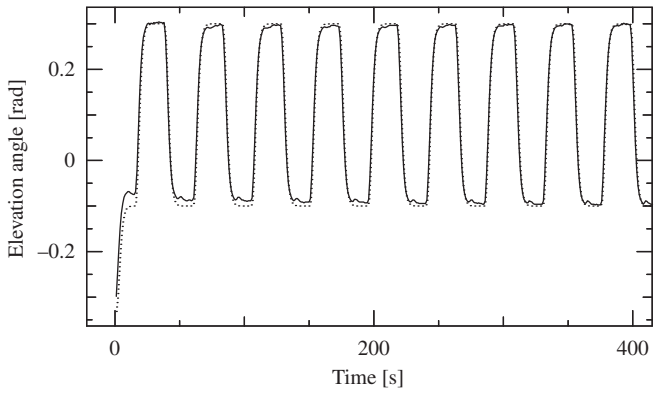

Fig. 9. The time evolution of angle ε (—) and reference output ε_M (···).

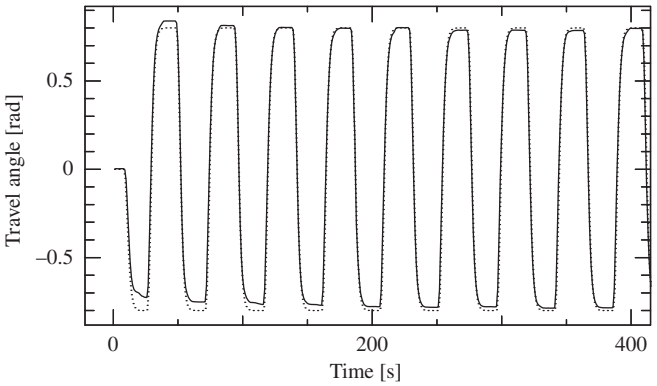

Fig. 10. The time evolution of angle ϕ (—) and reference output ϕ_M (···).

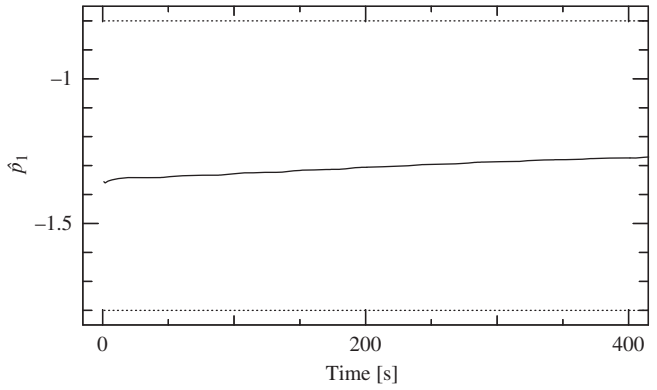

Fig. 11. Time evolution of the estimated parameter $\hat{p}_1$. The dotted lines represent the limiting values.

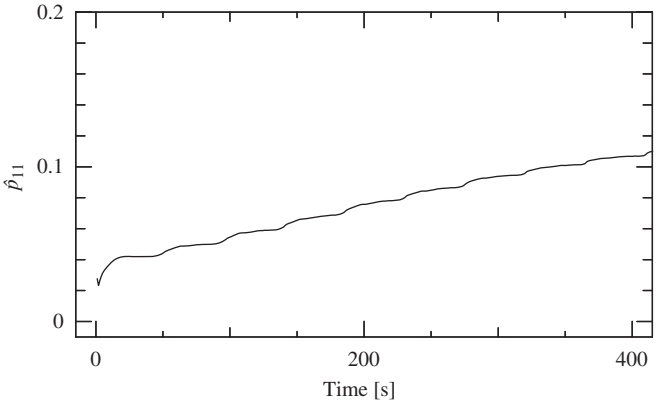

Fig. 12. Time evolution of the estimated parameter $\hat{p}_{11}$.

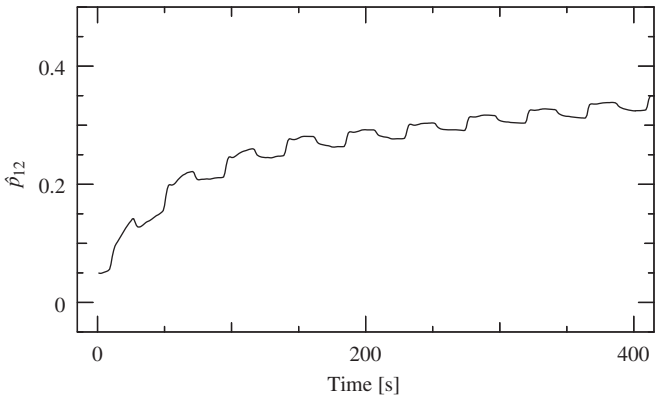

Fig. 13. Time evolution of the estimated parameter $\hat{p}_{12}$.

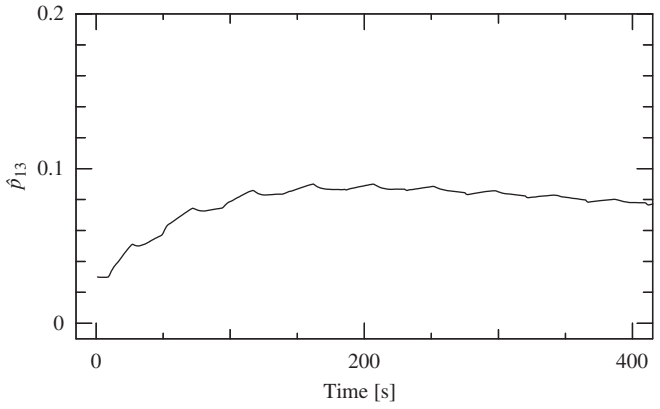

Fig. 14. Time evolution of the estimated parameter $\hat{p}_{13}$.

and the system parameters $\hat{\xi}_i(k)$ can be identified by the recursive least squares algorithm (20) and (21) based on expression (34).

5.2.2. Experimental studies

The design parameters and the reference model are the same as those of the previous section. The outputs are depicted in Figs. 9 and 10, while the estimated parameters are shown in Figs. 11–14.

The tracking performance of both of the outputs ε and ϕ has been further improved by the inclusion of the uncertainties. Most of the estimated parameters, however, do not seem to converge to constant values. The reason is that the parameters move slightly in order to suppress the effect of the modelling error since there still remain further unmodelled dynamics.

6. Conclusions

This paper considers the nonlinear adaptive model following control of a 3-DOF model helicopter. The system model here is not decouplable by static state feedback, and the nonlinear structure algorithm is applied. When a simple model following controller is designed, it is not easy to obtain a good control performance mainly due to the parameter uncertainties. Then, two parameter identification schemes are discussed: the first scheme is based on the differential equation model. This scheme is unable to obtain a good tracking control performance because of the inaccuracy of the estimated velocity and acceleration signals. The second scheme is designed for a dynamics model derived by applying integral operators to the differential equations expressing the system dynamics. Hence, this identification algorithm requires neither velocity nor acceleration signals. The experimental results show that the second method yields a better tracking objective, although tracking errors still remain. Finally, extra terms are introduced into the equations of motion to express model uncertainties and external disturbances. With reference to experimental results, this modification is shown to further improve the tracking control performance.

For the future work, development and application of digital controller designs based on a sampled-data model for the nonlinear helicopter is left.

Acknowledgements

The authors would like to thank the anonymous reviewers for helpful comments to improve the manuscript.

References

Apkarian, J. (1998). *3D Helicopter experiment manual*. Canada: Quanser Consulting.
Chakrabortty, A., Arcak, M., & Tsiotras, P. (2008). Robust design of a spacecraft attitude tracking control system with actuator uncertainties. In *Proceedings of the 47th IEEE conference on decision and control* (pp. 1587–1592).
Dzul, A., Hamel, T., & Lozano, R. (2002). Nonlinear control for a tandem rotor helicopter. In *Preprints of the 15th IFAC triennial world congress* (pp. 305–313).
Goodwin, C. G., & Sin, S. K. (1984). *Adaptive filtering, prediction and control. Information and system science series*. USA: Prentice-Hall.
Hu, C., Zhu, J., Huang, X., Hu, J., & Sun, Z. (2004). Output tracking of an unmanned tandem helicopter based on dynamic augment method. *International Journal of Control, Automation and Systems*, *2*(2), 156–164.
Isidori, A. (1995). *Nonlinear control systems* (3rd ed.). USA: Springer Verlag.
Isurugi, Y. (1990). *Model following control for nonlinear systems*. INRIA Reports, No. 1332.
Kim, H. J., & Shim, D. H. (2003). A flight control system for aerial robots: Algorithms and experiments. *Control Engineering Practice*, *11*(12), 1389–1400.
Koo, T. J., & Sastry, S. (1998). Output tracking control design of a helicopter model based on approximate linearization. In *Proceedings of the 37th IEEE conference on decision and control* (pp. 3596–3601).
Krstic, M., Kanellakopolous, I., & Kokotovic, P. V. (1995). *Nonlinear and adaptive control design*. USA: Wiley.
Kutay, A. T., Calise, A. J., Idan, M., & Hovakimyan, N. (2005). Experimental results on adaptive output feedback control using a laboratory model helicopter. *IEEE Transactions on Control Systems Technology*, *13*(2), 196–202.
Mahony, R., & Hamel, T. (2004). Robust trajectory tracking for a scale model autonomous helicopter. *International Journal of Robust and Nonlinear Control*, *14*(12), 1035–1059.
Marconi, L., & Naldi, R. (2007). Robust full degree-of-freedom tracking control of a helicopter. *Automatica*, *43*(11), 1909–1920.
Postlethwaite, I., Prempain, I., Turkoglu, E., Tuner, M. C., Ekkis, K., & Gubbels, A. W. (2005). Design and flight testing of various h-infinity controllers for the bell 205 helicopter. *Control Engineering Practice*, *13*(3), 383–398.
Shima, M., Isurugi, Y., Yamashita, Y., Watanabe, A., Kawamura, T., & Yokomichi, M. (1997). *Control theory of nonlinear systems*. Japan: Corona Publishing (in Japanese).
Singh, N. S. (1981). A modified algorithm for invertibility in nonlinear systems. *IEEE Transactions on Automatic Control*, *13*(2), 196–202.
Sira-Ramirez, H., Zribi, M., & Ahmad, S. (1994). Dynamical sliding mode control approach for vertical flight regulation in helicopters. *IEE Proceeding Control Theory and Application*, *141*(1), 19–24.
Spong, M. W., Lewis, F., & Abdallah, C. (1992). *Robot dynamics and control: Dynamics, motion planning, and analysis*. USA: IEEE Press.
Tao, G. (2003). *Adaptive control design and analysis*. USA: Wiley.
Trentini, M., & Pieper, J. K. (2001). Mixed norm control of a helicopter. *AIAA Journal of Guidance, Control, and Dynamics*, *24*(3), 555–565.